Acta Crystallographica Section F
Structural Biology and Crystallization Communications
ISSN 1744-3091

Cloning, expression, purification, crystallization and preliminary crystallographic analysis of pseudo death-effector domain of HIPPI, a molecular partner of Huntingtin-interacting protein HIP-1

Manisha Banerjee, Pritha Majumder, Nitai P. Bhattacharyya, Jiban K. Dattagupta and Udayaditya Sen*

Structural Genomics Section, Saha Institute of Nuclear Physics, 1/AF Bidhan Nagar, Kolkata 700064, India

Correspondence e-mail: udayaditya.sen@saha.ac.in

Received 8 September 2006
Accepted 6 November 2006

The formation of a heterodimer between Huntingtin-interacting protein-1 (HIP-1) and its novel partner HIPPI (HIP-1 protein interactor) through their pseudo death-effector domains (pDEDs) is a key step that recruits caspase-8 and initiates apoptosis. This could be one of the pathways by which apoptosis is increased in Huntington's disease (HD). A construct consisting of the pDED of HIPPI has been cloned and overexpressed as 6NH-tagged protein and purified by Ni–NTA affinity chromatography. Crystals of the pDED of HIPPI were grown in space group $P4_1$, with unit-cell parameters $a = b = 77.42$, $c = 33.31$ Å and a calculated Matthews coefficient of 1.88 Å^3 Da^{-1} (33% solvent content) with two molecules per asymmetric unit.

1. Introduction

Huntington's disease (HD; MIM 143100) is an autosomal dominant neurodegenerative disorder caused by the expansion of polymorphic CAG repeats beyond 37 in the coding sequence of the *huntingtin* (*Htt*) gene (The Huntington's Disease Collaborative Research Group, 1993). The prevalence of the disease varies worldwide, being very common in certain Caucasian populations (Harper, 1991; Narabayashi, 1973). It is believed that the increased number of glutamines to beyond 40 in the N-terminal region of the protein Huntingtin (Htt) leads to selective neuronal loss through the process of increased apoptosis (reviewed in Young, 2003). However, the detailed molecular pathways that explain the correlation between the expansion of the polyglutamine repeat within Htt and subsequent neurodegeneration are unclear. A large number of specialized proteins, mostly modular in structure, have been identified that purposefully interact in a coordinated manner to ensure the correct execution of the apoptotic process (Li & Li, 2004). One of these modules is the death-effector domain (DED), which is predominantly found in the components of death-inducing signalling complexes, which facilitate the assembly of protein components required for the execution of various cell-death pathways. Death-effector domain (DED) containing proteins facilitate the selective homo- or hetero-dimerization of proteins and play a pivotal role in diverse cellular functions, including apoptosis through receptor signalling (Barnhart *et al.*, 2003; Wanker, 2002). DED-containing proteins such as DEDD (death-effector domain proteins that DNA) have also been reported to bind DNA and inhibit RNA polymerase I activity *in vivo* and to regulate transcription (Schickling *et al.*, 2001; Zhan *et al.*, 2002).

Huntingtin-interacting protein-1 (HIP-1), which is expressed mainly in the central nervous system, has been identified through its interaction with Htt. HIP-1 and Htt are co-localized to clathrin-coated vesicles (Metzler *et al.*, 2001), indicating their role in endocytosis. HIP-1 has recently been shown to contain a pseudo death-effector domain (pDED) motif and, similar to all other DED-

containing proteins, overexpression of HIP-1 induces apoptosis (Hackam *et al.*, 2000). In HD, Htt has significant less affinity for HIP-1, resulting in the availability of free pDED-containing HIP-1 protein, which might trigger a new apoptotic pathway (Gervais *et al.*, 2002).

A yeast two-hybrid screen was performed to search for the interacting partners of HIP-1, which identified the protein HIPPI (HIP-1 protein interactor; Gervais *et al.*, 2002). HIPPI is a 429-amino-acid protein and the C-terminal region (residue 335–426) of HIPPI contains a pseudo DED-like motif. The domain organizations of HIPPI and HIP-1 are shown in Fig. 1. The pDED domain of HIPPI (hereafter termed pDED-HIPPI) exhibits 39.2% similarity and 26.6% identity to the pDED of HIP-1 (hereafter called pDED-HIP-1) in amino-acid sequence. Moreover, pDED-HIPPI shows only 34.9% similarity and 21% identity to other known DEDs. It is believed that the interaction of HIP-1 with HIPPI is carried out through the pDED domains present in both proteins. pDED differs from its conformational neighbour DED by the presence of charged residues at the interacting helices in contrast to the hydrophobic amino acids in DED (Gervais *et al.*, 2002). It is interesting to note that an alignment of all known DED domains failed to align pDED-HIPPI (Barnhart *et al.*, 2003), indicating the dissimilarity between the various known DED domains.

HIP-1 and HIPPI form a heterodimer through their pDED domains and the formation of this heterodimer (HIPPI–HIP-1) is favoured by the presence of Htt having an expanded polyglutamic repeat. This complex then recruits the initiator caspase-8 and activates the enzymes for apoptosis (Gervais *et al.*, 2002; Majumder *et al.*, 2006). This cellular model provides an alternative explanation for the increased apoptosis observed in HD and deviates slightly from the earlier model, in which aggregates formed by the mutated Htt recruit caspase-8 and initiate apoptosis (Sánchez *et al.*, 1999). Recently, we have shown that exogenous expression of HIPPI in Neuro2A neuronal cells increases apoptosis by activating caspase-1 and caspase-3 and releasing cytochrome *c* from mitochondria. We have also reported that caspase-1, caspase-8, caspase-9/caspase-6 and caspase-3 activation and nuclear fragmentation were increased significantly when HIPPI was overexpressed in HeLa and Neuro2A cells (Majumder *et al.*, 2006).

To date, no homologous structure for pDED-HIPPI or pDED-HIP-1 has been reported. With the ultimate goal of identifying the structural basis of the interactions between HIPPI and HIP-1 and the way the pDED differs from other DED domains, we here report the cloning, expression, purification, crystallization and preliminary X-ray analysis of pDED-HIPPI.

2. Materials and methods

2.1. Cloning, expression and purification of pDED-HIPPI

The pDED-HIPPI gene was cloned in pPROTet C1 vector (BD Bioscience, USA) using specific primers (forward, 5′-**ACGCGTC-GAC**GTCGGAAATGGAGGAGTGACGG-3′; reverse, 5′-**CGGG-ATCC**CGTTAATAAAAGCCTGTTGCTGGTT-3′). The primers were synthesized with adaptors (bold) for the restriction enzymes *Sal*I and *Bam*HI (MWG Biotech, Germany). HIPPI, cloned in pGEFP, was used as a DNA template to amplify the region encoding pDED. The amplified ORF was purified (Qiagen) from 1.5% agarose gel, digested with *Sal*I and *Bam*HI (Promega, USA) and then ligated with pPROTet C1 vector (BD Bioscience, USA) previously digested with the same restriction enzymes. The ligated product was transformed into competent strain DH5α and plasmid DNA was isolated from colonies. The clone was confirmed by DNA sequencing and restriction-enzyme digestion.

The pPROTet construct was transformed into competent bacterial strain BL21Pro and was selected on a chloramphenicol (HiMedia) LB agar plate. A single colony was picked and transferred into 100 ml LB broth and grown overnight. A 1% inoculum was seeded into 1 l LB broth from the previous culture and grown at 310 K until OD_{600} reached 0.6; the cells were then induced with 100 ng l^{-1} anhydro tetracycline (IBA Germany). After overnight induction at 293 K, cells were harvested at 4500*g* for 20 min and the pellet was stored at 193 K. The cell pellet was resuspended in 25 ml ice-cold lysis buffer (20 m*M* Tris–HCl pH 8, 150 m*M* NaCl, 1 m*M* PMSF, 5 m*M* imidazole) and lysed by sonication on ice. Cell lysate was then centrifuged (12 000*g* for 30 min) at 277 K and the supernatant containing pDED was purified using an Ni–NTA column (Qiagen). The 6NH-tagged pDED protein was eluted with 250 m*M* imidazole (Sigma) and the purity of the eluted fractions was checked by 15% SDS–PAGE (Fig. 2); the protein was found to be nearly homogeneous. The eluted protein was first dialyzed overnight against 0.1 *M* Tris–HCl pH 8.0 containing 100 m*M* NaCl and then against 0.1 *M* Tris–HCl pH 8.0 containing 50 m*M* NaCl. At this stage, slight precipitation of the protein was observed and the precipitated protein was centrifuged. The precipitate and the supernatant were run separately on a 15% SDS–PAGE. The lanes containing the precipitate showed the majority of the

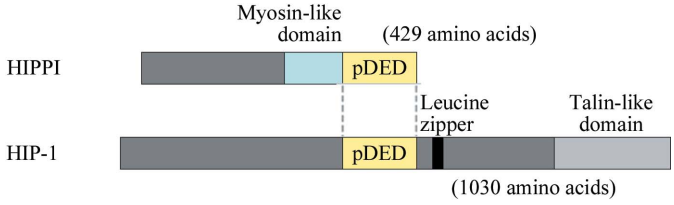

Figure 1
Schematic diagram showing the organization of HIPPI and HIP-1. The pDED domain in HIPPI and HIP-1 is shown in yellow and labelled, while the other domains are in different colours.

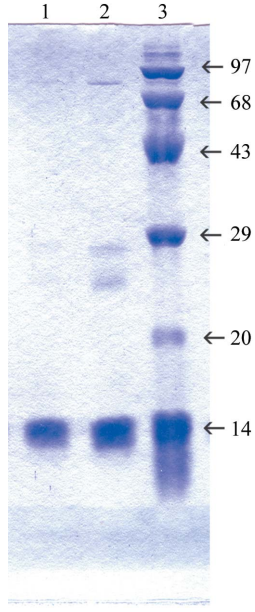

Figure 2
15% SDS–PAGE of pDED-HIPPI eluted after Ni–NTA affinity chromatography. Lanes 1 and 2, fractions containing pDED-HIPPI; lane 3, molecular-weight markers (kDa).

Table 1
Data-collection and data-processing parameters of pDED.

Values in parentheses are for the last shell.

Space group	*P*4
Unit-cell parameters (Å)	$a = b = 77.42$, $c = 33.31$
Oscillation range (°)	0.5
Maximum resolution (Å)	2.2 (2.3–2.2)
No. of molecules per ASU	2
Matthews coefficient (V_M; Å^3 Da^{-1})	1.88
Solvent content (%)	33.0
No. of observations	60404
No. of unique reflections	5917
Mosaicity	0.28
Completeness (%)	99.8 (98.8)
R_{merge}† (%)	6.6 (22.9)
$I/\sigma(I)$ in last shell	2.3

† $R_{merge} = \sum[\sum |I(h)_i - I(h)|]/\sum I(h)$, where $I(h)_i$ is the observed intensity of the ith measurement of reflection h and $I(h)$ is the mean intensity of reflection h calculated after scaling.

contaminant proteins, while the supernatant contained the desired 6NH-tagged pDED protein with more than 90% purity.

2.2. Crystallization

For crystallization, the intact 6NH-tagged pDED-HIPPI protein was dialyzed against 20 m*M* Tris–HCl pH 8.0 containing 200 m*M* NaCl and concentrated with Amicon Centriprep centrifugal filtration units (MWCO 10 000 Da) to 12 mg ml^{-1}. Crystallization was performed by the hanging-drop vapour-diffusion method using 24-well tissue-culture plates. Grid Screen Ammonium Sulfate, Crystal Screen I and Crystal Screen II (Jancarik & Kim, 1991) were used to establish the initial crystallization conditions. Typically, 2 µl protein solution (12 mg ml^{-1}) was mixed with an equal volume of screening solution and equilibrated over 700 µl of the latter as reservoir solution. Crystals were observed under three different crystallization conditions and each promising crystallization condition was further optimized. The best crystals (0.5 × 0.35 × 0.3 mm; Fig. 3*a*) were obtained when 2 µl protein solution was mixed with an equal volume of reservoir solution containing 1.5 *M* ammonium sulfate, 2% PEG 4000 in 0.1 *M* sodium acetate buffer pH 4.6 (or 0.1 *M* Tris–HCl buffer pH 8.0) and equilibrated at 277 K for 10 d against the latter. A low-salt crystallization condition has also been found which contains 10% PEG 4000, 1% ammonium sulfate in 0.1 *M* Tris–HCl pH 8.0 and produced prism-shaped crystals of smaller size (0.2 × 0.15 × 0.15 mm; Fig. 3*b*).

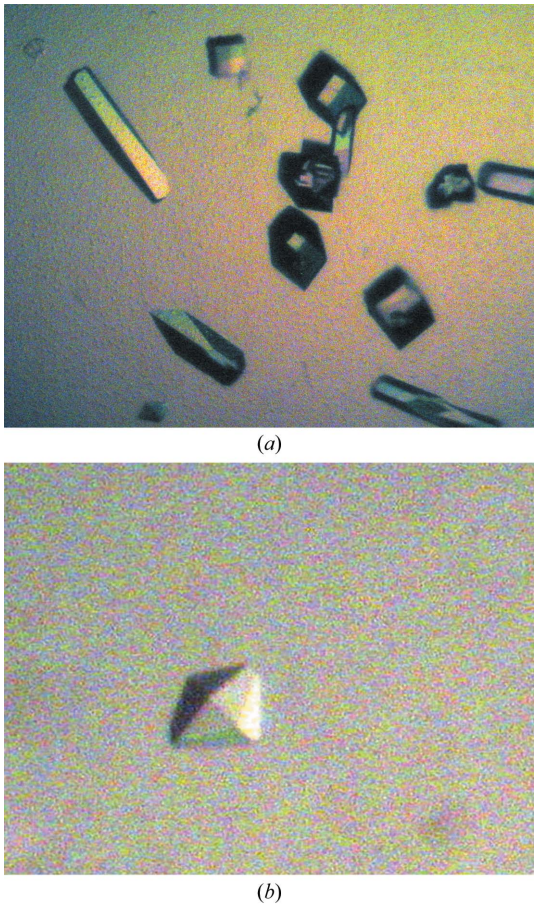

(*a*)

(*b*)

Figure 3
Crystals of pDED-HIPPI. (*a*) Crystals grown in the presence of a high-salt precipitant containing 1.5 *M* ammonium sulfate and 2% PEG 4000; (*b*) crystals grown in the presence of a low-salt precipitant containing 10% PEG 4000, 1% ammonium sulfate.

2.3. Data collection and processing

Crystals of pDED-HIPPI grown under high-salt condition (in the presence of 1.5 *M* ammonium sulfate) were fished out from the crystallization drops using a nylon loop (Hampton Research, Laguna Niguel, CA, USA), dipped in a solution of 1.3 *M* ammonium sulfate containing 15% glycerol and flash-frozen in a stream of nitrogen (Oxford cryosystem) at 100 K. X-ray diffraction data were collected to 2.2 Å resolution (Fig. 4) using a MAR Research image-plate detector (diameter 345 mm) and Cu $K\alpha$ radiation generated by a Bruker–Nonius FR591 rotating-anode generator equipped with Osmic MaxFlux confocal optics and running at 50 kV and 90 mA. A total of 320 frames were collected with a crystal-to-detector distance of 175 mm. The exposure time for each image was 2 min and the oscillation range was maintained at 0.5°. Data were processed and

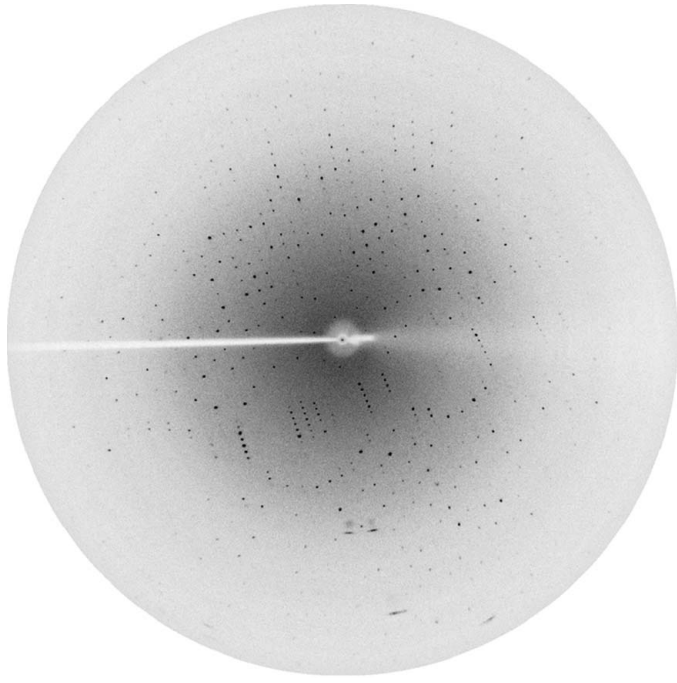

Figure 4
Diffraction image of the pDED-HIPPI crystal grown under high-salt conditions.

scaled using *AUTOMAR* (http://www.marresearch.com/automar/). Data-collection and processing statistics are given in Table 1.

3. Results

The crystals belong to the tetragonal space group $P4_1$, with unit-cell parameters $a = b = 77.42$, $c = 33.31$ Å. The results of molecular-weight determination of pDED-HIPPI by MALDI–TOF consistently gave a molecular weight of ∼13.4 kDa (see supplementary material[1]), which is in good agreement with the molecular weight calculated for the amino-acid sequence of the recombinant 6NH-tagged pDED protein. Based on the molecular weight of 13.4 kDa, packing considerations indicate the presence of two molecules in the asymmetric unit, which corresponds to a Matthews coefficient V_M (Matthews, 1968) of 1.88 Å^3 Da^{-1} and a solvent content of 33%. The low-salt crystals diffracted to 2.6 Å resolution and were isomorphous to the crystals grown in the presence of high-salt precipitant. Initially, we used these crystals to obtain heavy-atom derivatives, but subsequently the high-salt crystals were also used. High-salt crystals were gradually transferred to a 20% PEG 4000 solution prior to heavy-metal soaking and data were collected to 2.5 Å.

[1] Supplementary material has been deposited in the IUCr electronic archive (Reference: TB5005).

References

Barnhart, B. C., Lee, J. C., Alappat, E. C. & Peter, M. E. (2003). *Oncogene*, **22**, 8634–8644.

Gervais, F. G., Singaraja, R., Xanthoudakis, S., Gutekunst, C. A., Leavitt, B. R., Metzler, M., Hackam, A. S., Tam, J., Vaillancourt, J. P., Houtzager, V., Rasper, D. M., Roy, S., Hayden, M. R. & Nicholson, D. W. (2002). *Nature Cell Biol.* **4**, 95–105.

Hackam, A. S., Yassa, A. S., Singaraja, R., Metzler, M., Gutekunst, C. A., Gan, L., Warby, S., Wellington, C. L., Vaillancourt, J., Chen, N., Gervais, F. G., Raymond, L., Nicholson, D. W. & Hayden, M. R (2000). *J. Biol. Chem.* **275**, 41299–41308.

Harper, P. S. (1991). *Huntington's Disease.* London: W. B. Saunders.

Jancarik, J. & Kim, S.-H. (1991). *J. Appl. Cryst.* **24**, 409–411.

Li, S. H. & Li, X. J. (2004). *Trends Genet.* **20**, 146–154.

Majumder, P., Chattopadhyay, B., Mazumder, A., Das, P. & Bhattacharyya, N. P. (2006). *Neurobiol. Dis.* **22**, 242–256.

Matthews, B. W. (1968). *J. Mol. Biol.* **33**, 491–497.

Metzler, M., Legendre-Guillemin, V., Gan, L., Chopra, V., Kwok, A., McPherson, P. S. & Hayden, M. R. (2001). *J. Biol. Chem.* **276**, 39271–39276.

Narabayashi, H. (1973). *Advances in Neurology*, Vol. 1, edited by A. Barbeau, T. N. Chase & G. W. Paulson, pp. 253–259. New York: Raven Press.

Sánchez, I., Xu, C. J., Juo, P., Kakizaka, A., Blenis, J. & Yuan, J. (1999). *Neuron*, **22**, 623–633.

Schickling, O., Stegh, A. H., Byrd, J. & Peter, M. E. (2001). *Cell Death Differ.* **8**, 1157–1168.

The Huntington's Disease Collaborative Research Group (1993). *Cell*, **72**, 971–983.

Wanker, E. E. (2002). *Dev. Cell*, **2**, 126–128.

Young, A. B. (2003). *J. Clin. Invest.* **11**, 299–302.

Zhan, Y., Hegde, R., Srinivasula, S. M., Fernandes-Alnemri, T. & Alnemri, E. S. (2002). *Cell Death Differ.* **9**, 439–447.